Geomechanics and Engineering, *Vol. 25, No. 4 (2021) 341-345*
DOI: https://doi.org/10.12989/gae.2021.25.4.341

Investigation of 1D sand compression response using enhanced compressibility model

Song-Hun Chong*

Department of Civil Engineering, Sunchon National University, 255 Jungang-ro, Sunchon, Jeollanam-do 57922, Republic of Korea

(Received January 19, 2021, Revised April 1, 2021, Accepted May 13, 2021)

Abstract. 1D sand compression response to ko-loading experiences volume contraction from low to high effective stress regimes. Previous study suggested compressibility model with physically correct asymptotic void ratios at low and high stress levels and examined only for both remolded clays and natural clays. This study extends the validity of Enhanced Terzaghi model for different sand types complied from 1D compression data. The model involved with four parameters can adequately fit 1D sand compression data for a wide stress range. The low stress obtained from fitting parameters helps to identify the initial fabric conditions. In addition, strong correlation between compressibility and the void ratio at low stress facilitates determination of self-consistent fitting parameters. The computed tangent constrained modulus can capture monotonic stiffening effect induced by an increase in effective stress. The magnitude of tangent stiffness during large strain test should not be associated with small strain stiffness values. The use of a single continuous function to capture 1D stress-strain sand response to ko-loading can improve numerical efficiency and systematically quantify the yield stress instead of ad hoc methods.

Keywords: 1D sand compression response; enhanced Terzaghi model; monotonic stiffening effect; tangential stiffness; small strain stiffness; yield stress

1. Introduction

Generally, soil compressibility that relates the effective stress to volume change is used to predict the approximate settlement. Standard settlement analyses assume recompression and normal compression segments before and after the yield stress σ'_y. Several graphical methods have been proposed to determine the yield stress or preconsolidation pressure (Casagrande 1936, Janbu 1969, Becker *et al.* 1987, Sridharan *et al.* 1991, Clementino 2005, Boone 2010). However, the use of two compression functions as constitutive equation requires high numerical cost to quantify the elastic and plastic deformation. Thus, a single function is needed to capture the complete compression response and streamline computations.

One dimensional sand compression response to k_o-loading undergoes volume contraction. It exhibits extremely low, extremely high effective stress, or a wide effective stress range. Examples include: suction casings - (Houlsby *et al.* 2005); skirted foundation - (Bransby and Randolph 1998), migration of pipelines (Krost *et al.* 2011, Randolph *et al.* 2011); pile tips (Yang *et al.* 2010, Tsuha *et al.* 2012), blast loads (Wang *et al.* 2005). Chong and Santamarina (2016) compiled previously suggested models and other functions to satisfy physically correct asymptotic values at low stress $\sigma' \rightarrow 0$ and high stresses $\sigma' \rightarrow \infty$. All four-parameter models are fitted for both remolded clays and natural clays. This paper attempts to test enhanced compressibility model for sand and investigate the effect of sand properties on 1D sand compression response.

*Corresponding author, Professor
E-mail: shchong@scnu.ac.kr

2. Enhanced compressibility model

From low to high stress regime. Individual particles form a granular skeleton with a characteristic finite porosity. Compressibility at low stress reflects degree of cementation during diagenetic process (Yun and Santamarina 2005), initial packing density and particle shape (Pestana and Whittle 1995, Cho *et al.* 2006), and fine contents (DeJong and Christoph 2009, Hyodo *et al.* 2017). Those initial sand fabric conditions still influence 1D soil compression behavior response at this intermediate stress regime. For example, higher initial packing density or more fine contents reduces the curvature of the compression curves. At high stress regime, particle compliance, crushing, and creep are the prevailing deformation mechanisms at high stress (Hagerty *et al.* 1993, Nakata *et al.* 2001, Wang and Wong 2010). Past history loses relevance regardless of the initial particle properties unless particle crushing produces a different particle shape and grain size distribution.

Enhanced Terzaghi model. The classical semi-logarithmic model has been widely used to calculate the settlement in geotechnical engineering $e = e_c - C_c \cdot \log(\sigma'/\sigma'_c)$. This function involved with two parameters (e_c and C_c) fits well 1D sand compression at intermediate stress levels, yet predicts $e \rightarrow \infty$ as $\sigma'_z \rightarrow 0$ and $e<0$ as $\sigma'_z \rightarrow \infty$. Asymptotic void ratios e_L at low stress and e_H at high

ISSN: 2005-307X (Print), 2092-6219 (Online)

stress can be imposed into classical Terzaghi equation to benefit from the accumulated knowledge in the field. While the lower compressibility at high stress requires higher order terms to improve the fitting of experimental data, model parameters should include the clear physical meanings. Thus, the enhanced Terzaghi model is modified to satisfy asymptotic conditions: $e \to e_L$ as $\sigma' \to 0$, and $e \to e_H$ as $\sigma' \to \infty$ as

$$e = e_{ref} - C_c \log\left(\frac{\sigma'_{ref}}{\sigma' + \sigma'_L} + \frac{\sigma'_{ref}}{\sigma'_H} \right)^{-1} \quad (1)$$

where reference void ratio e_{ref} and Compression index Cc determine the trend within the intermediate stress levels. The reference effective stress σ'_{ref} = 1 MPa is selected because the yield stress in 1D compression data occurs near that stress level. The lower and upper void ratio plateaus e_L and e_H that correspond to the asymptotic stresses σ'_L and σ'_H are obtained by imposing each stress boundary condition into Eq. (1).

$$\sigma'_H = 10^{\frac{e_{ref} - e_H}{C_c}} \cdot \sigma'_{ref} \quad \text{when } \sigma' \to \infty \quad (2)$$

$$\sigma'_L = \frac{\sigma'_H}{10^{\frac{e_L - e_H}{C_c}} - \sigma'_{ref}} \cdot \sigma'_{ref} \quad \text{when } \sigma' \to 0 \quad (3)$$

In addition, the tangent constrained modulus can be computed from enhanced compressibility model by taking derivative to define incremental void ratio and effective stress as

$$M_{tan} = \lim_{\Delta\varepsilon \to 0} \frac{\sigma'(\varepsilon + \Delta\varepsilon) - \sigma'(\varepsilon)}{\Delta\varepsilon} = \frac{\partial\sigma'}{\partial\varepsilon} = 2.3\frac{(1+e)}{C_c}(\sigma' + \sigma'_L)\cdot\left(1 + \frac{\sigma' + \sigma'_L}{\sigma'_H}\right) \quad (4)$$

Note that the tangent stiffness provides continuous assessment which is unaffected by errors (e.g., unstable measurements) and improves the data interpretation (Atkinson *et al.* 1986).

Other models. Models expressed with exponent term ($e - \sigma'^{\beta}$) are generalized by satisfying asymptotic conditions relevant to 1D soil compression data. The power function involved with four parameters was inspired by Boyle-Mariotte's law that ignores the size of molecules, which resembles loosely packed small particles. Gompertz function as one example of exponential functions was adapted to satisfy low-stress void ratio eL and high-stress void ratio eH. In particular, the hyperbolic model that has been extensively used to exhibit the prepeak deviatoric stress versus strain data was modified to capture 1D compressibility data in terms of $e - \sigma'$.

3. Results and discussion

Model examination. 1D sand compression data gathered for a wide stress range are fitted using the enhanced semi-logarithmic model for sands with different particle shape, particle size distribution (mean particle size), and initial packing density. The sand properties are tabulated with fitting parameters (Table 1). The data was compiled from Pestana and Whittle (1995). The 1D compression data and trends are shown in semi-log scale plot. Corresponding trends for the tangent constrained modulus are shown for four different sands. Additionally, the x and y axes are normalized with asymptotic low stress σ'_L and low-stress void ratio e_L obtained from the experimental data fitting. It can be observed that:

Table 1 Sand properties and fitting Parameters (Refer to data presented in Fig. 1). The data was compiled from Pestana and Whittle (1995)

Soil type	D50	Cu	e_{max}	e_{min}	Particle shape	e_L	e_H	e_{1MPa}	Cc	Error [%]
Quiou sand	0.7	4.5	1.2	0.78	Angular	1.01	0.1	1.06	0.46	0.2
	0.7	4.5			Angular	0.905	0.1	1.06	0.46	0.04
	0.7	4.5			Angular	0.815	0.1	1.06	0.46	0.02
Feldspar sand	0.6	1.5	1.1	0.89	Angular	1.1	0.1	1.24	0.55	0.5
	0.6	1.5			Angular	1.1	0.1	1.24	0.55	0.2
	0.6	1.5			Angular	1.1	0.1	1.24	0.55	0.34
Ottawa sand	0.14	1.5	0.82	0.65	Rounded	0.805	0.1	4.1	2.0	0.2
	0.14	1.5			Rounded	0.745	0.1	4.1	2.0	0.06
	0.14	1.5			Rounded	0.660	0.1	4.1	2.0	0.12
	0.28	1.5			Rounded	0.737	0.1	4.7	2.3	0.13
	0.6	1.5			Rounded	0.6	0.1	5	2.7	0.07
Quartz sand	0.08	1.8	1.05	0.81	Sub-rounded	0.845	0.1	1.95	0.9	0.16
	0.14	1.5			Sub-rounded	1.10	0.1	1.98	1.0	0.3
	0.28	1.5			Sub-rounded	1.07	0.1	2.10	1.1	0.24
	0.6	1.5			Sub-rounded	1.0	0.1	2.2	1.4	0.18

• Enhanced Terzaghi's model involved with four parameters can adequately fit experimental data gathered for four different sands [Fig. 1(a)]. Initial loose packing produces higher rate of change with increasing vertical stress level, and eventually converges towards the unique trend at high stress regime; at the same sand, initial fabric effect gradually diminishes. However, the severe particle crushing may produce different particle shape and grain size distribution and eventually exhibit complex 1D compression behavior (Hyodo *et al.* 2017)

• The results of computed tangent stiffness are plotted with log-log scale. The tangent constrained modulus increases with vertical effective stress due to monotonic stiffening effect in all cases [Fig. 1(b)]. It should tell the difference between small strain stiffness and large strain stiffness during concurrent large strain. The tangent stiffness calculated from stress-strain measurement is a mathematical concept that reveals the instantaneous rate of fabric change during a large strain test. By contrast, a "small-strain" perturbation test gives a constant fabric stiffness that is determined by contact deformation (Chong 2014).

• The normalization of the compression datasets shows

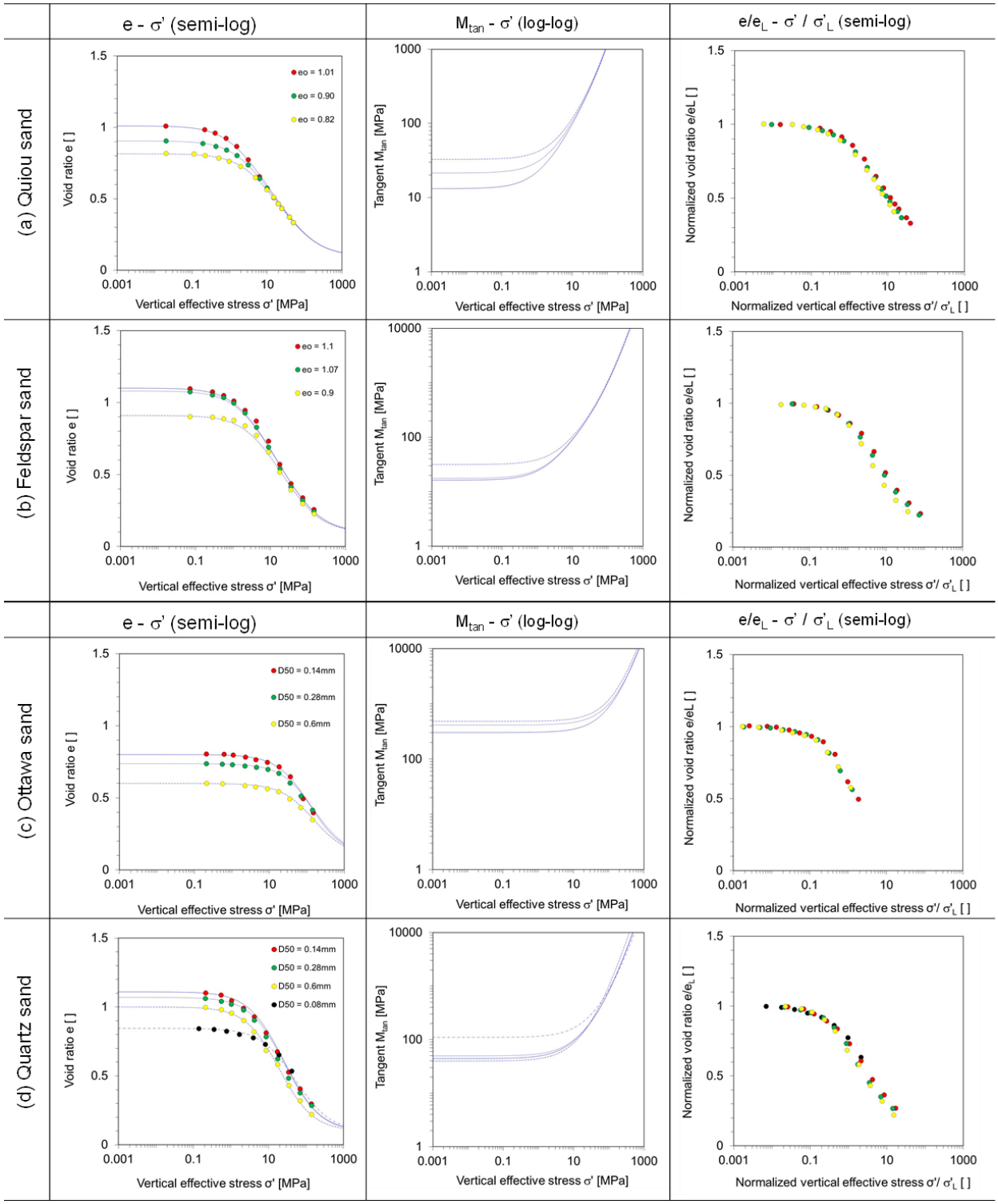

Fig. 1 Sand response under zero lateral boundary condition. The data is fitted with the Enhanced Terzaghi compressibility model involved with four physically meaningful parameters. (a) Quiou sand, (b) Feldspar sand, (c) Ottawa sand and (d) Quartz sand. The fitting parameters are tabulated on Table 1. The data from Pestana and Whittle (1995)

unique trends from low-to high- stress level [Fig. 1(c)]. Fig. 2 presents the normalized sand compression curve with different particle shapes. The angular particle extends threshold effective stress; rounded particle produces the higher low stress and the value of normalized stress is low. This further data interpretation could be used to systematically quantify the yield stress or preconsolidation stress instead of ad hoc methods based on graphical data interpretation.

Low-stress and initial fabric conditions. Low stress level related to directly yield stress is investigated with initial fabric conditions (Fig. 3). Higher low-stress void ratio (i.e., relatively loose packing) decreases low stress level. In

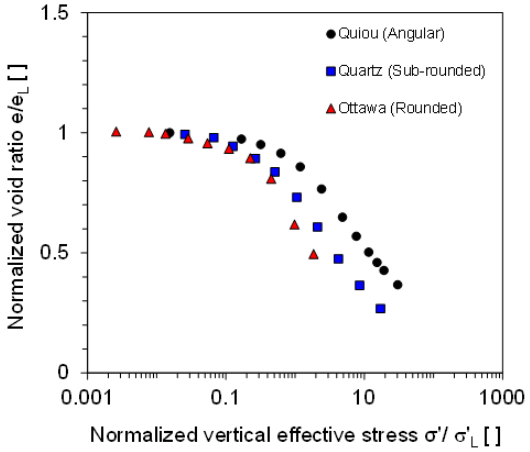

Fig. 2 Normalized 1D sand compression with different particle shapes. the x and y axes are normalized with asymptotic low stress σ'_L and low-stress void ratio e_L obtained from the experimental data fitting

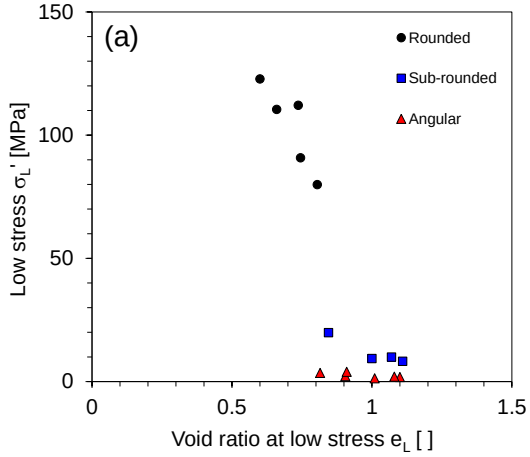

(a) Low-stress void ratio e_L for different particle shapes

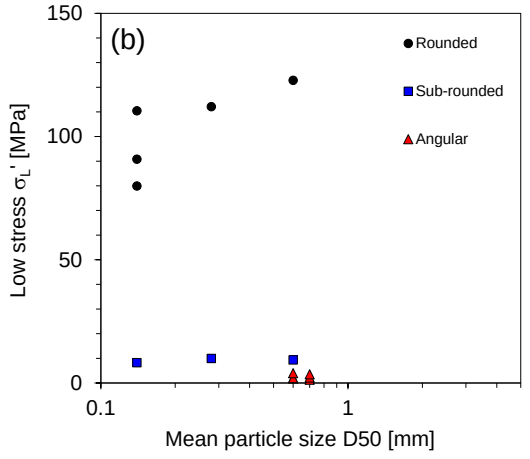

(b) Mean particle size D50 for different particle shapes

Fig. 3 Investigation of low stress obtained from model fitting on initial packing density, mean particle size, and particle shape

particular, the angular particle shape produces smaller low stress level at the same low-stress void ratio. This is because the particle irregularity hinders particle mobility and their ability to attain dense configuration, and thus

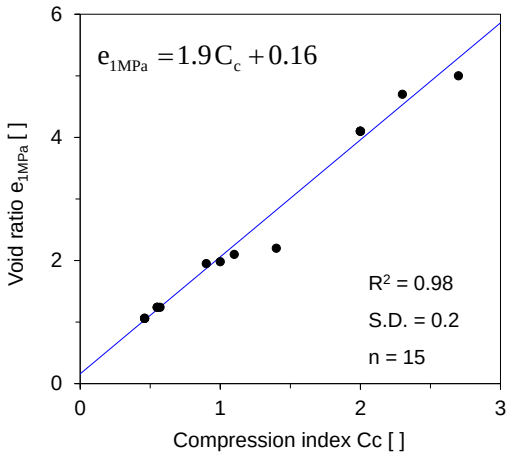

Fig. 4 Correlation between void ratio $e1_{MPa}$ and Cc for sands. S.D. indicates the standard deviation

unstable packing density develops earlier onset of yield stress. Meanwhile, mean particle size has little effect on the low stress level. Thus, the main sand properties influencing the low stress regime are initial packing density and particle shape. These trends were observed by Pestana and Whittle (1995).

Correlation - Low-stress void ratio and compressibility. The e_{1kPa} (void ratio at 1kPa) is required as constitutive model input parameter such as Modified Cam-Clay model. Chong and Santamarina (2016) proposed the empirical equation for remolded clays ($e_{1kPa} = 3.4 \cdot C_c + 0.48$). Also, this study obtains the correlation between model parameters e_{1MPa} and C_c (Fig. 4):

$$e_{1MPa} = 1.9 \cdot C_c + 0.16 \quad \textit{Sands} \text{ (15 cases, S.D = 0.2)} \quad (5)$$

Other compressibility models (power, exponential, hyperbolic, arctangent functions) that satisfy asymptotic void ratio at low and high stress levels can be tested for 1D sand compression data and establish the link between void ratio at low stress and compressibility.

Parameter invertibility. Least-square method is used to extract parameters by fitting the model with the 1D sand compression data. The error surface about the optimal parameter set is explored to evaluate the invertibility of each parameter by varying one parameter at the time. Limited data at very high stress causes poor convergence; model parameter can be constrained with a-priori data to restrict e_H. The reference void ratio e_{1MPa} is closely correlated with compressibility (Fig. 2). The constraint and correlations facilitate identifying a self-consistent set of fitting parameters, which implies that model complexity is reduced less than the four unknowns.

4. Conclusions

1D sand compression response shows the void ratio change from low to high effective stress regime. This study employs previously suggested a 1D compression model that

satisfies asymptotic conditions at low and high stress levels. The model can be used to fit the 1D sand compressibility response for sands with different particle shape, particle size distribution (mean particle size), and initial packing density. The following salient observation can be made:

• Enhanced Terzaghi model involved with four parameters can adequately fit 1D sand compression data gathered in a wide stress range. The low stress obtained from fitting parameters helps to identify the initial fabric conditions. In addition, strong correlation between compressibility and the void ratio at low stress facilitates determination of self-consistent fitting parameters.

• The computed tangent constrained modulus can capture monotonic stiffening effect induced by an increase in effective stress. It should be recognized that the magnitude of tangent stiffness during a large strain test is not be associated to small-stress stiffness values measured under constant fabric condition at the same e-σ' state.

• The use of a single continuous function to capture 1D stress-strain sand response to k_o-loading can improve numerical efficiency, facilitates computing the tangent constrained modulus, and systematically quantify the yield stress instead of ad hoc methods

Acknowledgments

This research was supported by the National Research Foundation of Korea (NRF) grant funded by the Korea government (MSIT) (No. 2021R1C1C1006003).

References

Atkinson, J.H., Richardson, D. and Woods, R.I. (1986), "Technical note on the determination of tangent stiffness parameters from soil test data", *Comput. Geotech.*, **2**(3), 131-140. https://doi.org/10.1016/0266-352X(86)90023-6.

Becker, D.E., Crooks, J.H.A., Been, K. and Jefferies, M.G. (1987), "Work as a criterion for determining in situ and yield stresses in clays", *Can. Geotech. J.*, **24**(4), 549-564. https://doi.org/10.1139/t87-070.

Boone, S.J. (2010), "A critical reappraisal of "preconsolidation pressure" interpretations using the oedometer test", *Can. Geotech. J.*, **47**(3), 281-296. https://doi.org/10.1139/T09-093.

Bransby, M.F. and Randolph, M.F. (1998), "Combined loading of skirted foundations", *Géotechnique*, **48**(5), 637-655. https://doi.org/10.1680/geot.1998.48.5.637.

Casagrande, A. (1936), "The determination of the pre-consolidation load and its practical significance", *Proceedings of the 1st International Soil Mechanics and Foundation Engineering Conference*, Cambridge, Massachusetts, U.S.A., June.

Cho, G.C., Dodds, J. and Santamarina, J.C. (2006), "Particle shape effects on packing density, stiffness, and strength: Natural and crushed sands", *J. Geotech. Geoenviron. Eng.*, **132**(5), 591-602. https://doi.org/10.1061/(ASCE)1090-0241(2007)133:11(1474).

Chong, S.H. (2014), "The effect of subsurface mass loss on the response of shallow foundations", Ph.D Disseration, Georgia Institute of Technology, Atlanta, Georgia, U.S.A.

Chong, S.H. and Santamarina, J.C. (2016), "Soil compressibility models for a wide stress range", *J. Geotech. Geoenviron. Eng.*, **142**(6), 06016003. https://doi.org/10.1061/(ASCE)GT.1943-5606.0001482.

Clementino, R.V. (2005), "Discussion: An oedometer test study on the preconsolidation stress of glaciomarine clays", *Can. Geotech. J.*, **42**(3), 972-974. https://doi.org/10.1139/t05-010.

DeJong, J. and Christoph, G. (2009), "Influence of particle properties and initial specimen state on one-dimensional compression and hydraulic conductivity", *J. Geotech. Geoenviron. Eng.*, **135**(3), 449-454. https://doi.org/10.1061/(ASCE)1090-0241(2009)135:3(449).

Hagerty, M., Hite, D., Ullrich, C. and Hagerty, D. (1993), "One-dimensional high-pressure compression of granular media", *J. Geotech. Eng.*, **119**(1), 1-18. https://doi.org/10.1061/(ASCE)0733-9410(1993)119:1(1).

Houlsby, G.T., Kelly, R.B., Huxtable, J. and Byrne, B.W. (2005), "Field trials of suction caissons in clay for offshore wind turbine foundations", *Géotechnique*, **55**(4), 287-296. https://doi.org/10.1680/geot.2005.55.4.287.

Hyodo, M., Wu, Y., Kajiyama, S., Nakata, Y. and Yoshimoto, N. (2017), "Effect of fines on the compression behaviour of poorly graded silica sand", *Geomech. Eng.*, **12**(1), 127-138. https://doi.org/10.12989/gae.2017.12.1.127.

Janbu, N. (1969), "The resistance concept applied to deformation of soils", *Proceedings of the 7th International Conference on Soil Mechanics and Foundation Engineering*, Mexico City, Mexico,

Krost, K., Gourvenec, S.M. and White, D.J. (2011), "Consolidation around partially embedded seabed pipelines", *Géotechnique*, **61**(2), 167-173. https://doi.org/10.1680/geot.8.T.015.

Nakata, Y., Hyodo, M., Hyde, A., Kato, Y. and Murata, H. (2001), "Microscopic particle crushing of sand subjected to high pressure one-dimensional compression", Japanese Geotechnical Society, Tokyo, Japan.

Pestana, J.M. and Whittle, A.J. (1995), "Compression model for cohesionless soils", *Géotechnique*, **45**(4), 611-631. https://doi.org/10.1680/geot.1995.45.4.611.

Randolph, M.F., Gaudin, C., Gourvenec, S.M., White, D.J., Boylan, N. and Cassidy, M.J. (2011), "Recent advances in offshore geotechnics for deep water oil and gas developments", *Ocean Eng.*, **38**(7), 818-834. https://doi.org/10.1016/j.oceaneng.2010.10.021.

Sridharan, A., Abraham, B.M. and Jose, B.T. (1991), "Improved technique for estimation of preconsolidation pressure", *Géotechnique*, **41**(2), 263-268. https://doi.org/10.1680/geot.1991.41.2.263.

Tsuha, C.H.C., Foray, P.Y., Jardine, R.J., Yang, Z.X., Silva, M. and Rimoy, S. (2012), "Behaviour of displacement piles in sand under cyclic axial loading", *Soils Found.*, **52**(3), 393-410. https://doi.org/10.1016/j.sandf.2012.05.002.

Wang, Z., Lu, Y., Hao, H. and Chong, K. (2005), "A full coupled numerical analysis approach for buried structures subjected to subsurface blast", *Comput. Struct.*, **83**(4-5), 339-356. https://doi.org/10.1016/j.compstruc.2004.08.014.

Wang, Z.C. and Wong, R.C.K. (2010), "Effect of grain crushing on 1D compression and 1D creep behavior of sand at high stresses", *Geomech. Eng.*, **2**(4), 303-319. http://doi.org/10.12989/gae.2010.2.4.303.

Yang, Z.X., Jardine, R.J., Zhu, B.T., Foray, P. and Tsuha, C.H.C. (2010), "Sand grain crushing and interface shearing during displacement pile installation in sand", *Géotechnique*, **60**(6), 469-482. https://doi.org/10.1680/geot.2010.60.6.469.

Yun, T. and Santamarina, J. (2005), "Decementation, softening, and collapse: Changes in small-strain shear stiffness in loading", *J. Geotech. Geoenviron. Eng.*, **131**(3), 350-358. https://doi.org/10.1061/(ASCE)1090-0241(2005)131:3(350).